

# Simulating Marine Current Turbine Wakes Using Advanced Turbulence Models

T. Ebdon<sup>\*†</sup>, D.M O’Doherty<sup>†</sup>, T. O’Doherty<sup>\*§</sup>, A. Mason-Jones<sup>\*¶</sup>

<sup>\*</sup>School of Engineering, Cardiff University, Cardiff, United Kingdom

<sup>†</sup>EbdonT@cardiff.ac.uk

<sup>§</sup>odoherty@cardiff.ac.uk

<sup>¶</sup>Mason-JonesA@cardiff.ac.uk

<sup>†</sup>School of Engineering, University of South Wales, Pontypridd, United Kingdom

daphne.odoherty@southwales.ac.uk

**Abstract**—Work is presented which compares the abilities of the Detached Eddy Simulation turbulence model to a Reynolds-Averaged Navier-Stokes turbulence model, for CFD simulations of a horizontal axis tidal turbine under different ambient turbulence conditions. Comparisons are made of the abilities of the respective models to predict both performance characteristics as well as wake length and character. It is demonstrated that whilst Detached Eddy Simulation holds little advantage over a  $k-\omega$  SST model for predicting mean performance characteristics, significant advantages are shown when predicting wake length, as well as allowing the prediction of the magnitude of fluctuations. It is expected that, despite the higher computational expense, hybrid LES-RANS turbulence models such as Detached Eddy Simulation will be of interest to engineers designing arrays of tidal turbines, which are anticipated if tidal energy is to make a significant contribution to the world’s energy resources.

## I. INTRODUCTION

Harnessing the power of tidal marine currents is seen as an increasingly important part of a move to lower-carbon energy production. Ocean scale models indicate that flows of high energy density exist over relatively small geographical areas[1]. In order to extract the maximum amount of energy and to allow tidal turbines to be economically viable, it is expected that turbines will be deployed in arrays in these areas of high flow energy. This grouping is not only advantageous from the point of view of energy extraction, but also allows for more efficient use of offshore infrastructure such as power conversion units, as well as for transport of the energy to land. If turbines are to be placed in close proximity to one-another, then it is inevitable that there will be hydrodynamic interactions between them. These could take the form of positive interactions, such as spanwise blockage of a channel leading to increased energy extraction[2][3], or negative interactions where downstream turbines operate in the wake of upstream turbines, or where the spanwise blockage is increased too much. In both scenarios, accurate forecasting of the production potential of a particular array configuration at a particular site is dependent on being able to accurately predict the flow around the turbine, taking into account both the energy extracted from the flow, as well the nature and extent of the wake.

It is therefore necessary to find a method of accurately predicting both the magnitude and character of the wake behind a tidal stream turbine, in order to produce optimised array layouts and to provide accurate calculation of the amount of power available from a given tidal channel. In addition to this, any turbine in the turbulent wake of an upstream device can be expected to experience fluctuating mechanical loads different to those experienced by a single turbine in a low-turbulence flow, with implications for the structural design of these devices.

Previous work has understandably focussed on turbine performance, and most of this work has been carried out using Reynolds Averaged Navier-Stokes (RANS) turbulence models and/or Blade Element Momentum Theory (BEMT) methods[4][5]. Various studies have been carried out to make

## NOMENCLATURE

$A$	=	rotor swept area, $m^2$
$C_{des}$	=	DES calibration constant
$C_P$	=	power coefficient
$C_T$	=	thrust coefficient
$C_\theta$	=	torque coefficient
$D$	=	rotor diameter, m
$F_{DES}$	=	DES turbulent kinetic energy dissipation multiplier
$F_t$	=	thrust force on turbine
$k$	=	turbulent kinetic energy
$L_t$	=	turbulent length scale
$r$	=	turbine radius, m
$\hat{x}$	=	unit vector in the $x$ direction
$\hat{y}$	=	unit vector in the $y$ direction
$\hat{z}$	=	unit vector in the $z$ direction
$y^+$	=	dimensionless wall coordinate
$\Delta_{max}$	=	local maximum cell dimension
$\delta_{ij}$	=	Kronecker delta
$\mu_t$	=	turbulent viscosity
$\rho$	=	fluid density
$\tau$	=	turbine torque
$\omega$	=	turbine angular velocity
$\omega$	=	specific dissipation rate
$Y_k$	=	turbulent kinetic energy dissipation term

predictions of  $C_P$ ,  $C_T$  and  $C_\theta$ , and these have shown reasonable accuracy when validated against experimental results for low turbulence flows. Attempts to predict the wake of horizontal axis tidal turbines (HATTs) have been made using RANS models for both tidal turbines[6], [7], as well as for wind turbines[8].

Studies measuring the turbulence at potential sites for tidal turbines[9] have demonstrated that realistic flows at such sites may be highly turbulent, and exhibit turbulent length scales of the same order of magnitude as the diameter of a turbine. Flume tank studies have shown the wake behind a HATT to be highly turbulent[10], with a high degree of anisotropy present in the turbulence in the wake[11]. These experimental results also indicate that the wake behind a HATT in highly turbulent flow conditions is significantly shorter than a pure RANS turbulence model might suggest. Taken together, it is reasonable to assume that HATTs can be expected to be deployed in highly turbulent environments, either due to high ambient turbulence or due to the wakes of other turbines in an array, and that improvement over RANS modelling is required to accurately predict wakes in these environments.

Numerical studies have been made using advanced turbulence modelling techniques such as Large Eddy Simulation (LES) in order to model turbines. The disadvantage of LES is the much larger associated computational costs, with these costs increasing particularly for high Reynolds number flows, due to the necessary high mesh densities in near-wall regions. Various attempts have been made to simplify turbine geometry to reduce the computational costs of these simulations. A study has been carried out using an LES method combined with a numerical particle emission method for 0% turbulence intensity case[12]. Actuator lines have been used to represent wind turbine blades in LES simulations, to explore the effect of the LES Sub-Grid Scale (SGS) model[13]. The actuator line approach is designed to reduce the computational cost associated with LES, by removing the need to fully resolve the boundary layer around turbine rotor blades. Another possible simplification is to represent the turbine as a porous actuator disc[14], again obviating the need for high mesh densities on the wall regions of turbine blades. This approach has been used in studies to examine the effect different turbulence intensities and length scales have on the wake behind these turbine simulators, and has shown that increases in turbulence intensity increase the rate of velocity recovery in the wake, and move the point of maximum velocity deficit closer to the disc. However, this simplification in geometry means that some details in the flow will not be modelled, such as blade-tip vortices, and, depending on they way the model is implemented, swirl in the wake.

The aim of the current study is to assess whether a hybrid LES/RANS scale-resolving turbulence model can more accurately represent the effects of turbulence on the wake of a HATT than pure RANS models, whilst simultaneously trying to keep computational costs to a minimum. With all simplifications, whether of geometry or of mathematical model, discretisation must be used to make simplifications which will have

the greatest benefit with regards to computational expense, whilst having the smallest effect on the flow prediction. In this study the authors have chosen to retain the full rotor geometry to allow the modelling of such flow features as tip vortices and swirl effects, but use Detached Eddy Simulation (DES) to reduce the mesh requirements and therefore computational expense. As the rate of velocity recovery in the wake is dependent on the mixing between the high-energy free stream and the low energy wake flows, and this in turn is dependent on the nature of the turbulence, it is postulated that a scale resolving turbulence model might improve the accuracy of wake predictions. The results from this LES/RANS hybrid turbulence model have been compared to those obtained using a pure RANS turbulence model. Simulations have been carried out for three different turbulence intensity levels, as previous experimental work[15][16] and LES simulations[14] has shown the importance of free stream turbulence on the nature and extent of a tidal turbine wake.

## II. SIMULATION METHODOLOGY AND CFD MODEL

The simulations carried out in this work were all conducted using the commercial software ANSYS Fluent®.

### A. Detached Eddy Simulation

Traditionally, CFD modelling of HATTs has used RANS turbulence models. RANS models have been the mainstay of CFD for many decades due to their computational efficiency and their applicability to a wide variety of flows. There are various schemes of differing complexity, ranging from one equation models such as the mixing length model, through two equation models such as the k- $\epsilon$  and k- $\omega$  models, to models such as the Reynolds Stress Model (RSM), which require seven transport equations to be solved for closure in 3 dimensions. Whilst the computational efficiency of RANS turbulence models is very appealing, they have some weaknesses which make them inappropriate for the modelling of the type of flow in the wake of a HATT under realistic turbulence conditions.

RANS turbulence models seek to take account of the effect of turbulence on the mean flow via the process of Reynolds decomposition. This decomposes an instantaneous flow variable such as velocity,  $u$ , into the sum of a mean,  $\bar{u}$ , and a fluctuating,  $u'$ , component:  $u = \bar{u} + u'$ . When these decomposed variables are substituted into the instantaneous Navier-Stokes equations, a new term appears, representing the transport of momentum between the turbulent eddies and the mean flow. These are known as the Reynolds stresses, have the form (using suffix notation) of  $\tau_{ij} = -\rho \overline{u'_i u'_j}$ , and must be modelled in order to close the Navier-Stokes equations. The different RANS turbulence models named above take different approaches to the modelling of the Reynolds stresses, with all but the seven equation RSM model relying on the Boussinesq approximation, which attempts to model the Reynolds stresses by relating them to the mean deformation rate:

$$\tau_{12} = \mu_t \left( \frac{\partial U_i}{\partial x_j} + \frac{\partial U_j}{\partial x_i} \right) - \frac{2}{3} \rho k \delta_{ij} \quad (1)$$

The Boussinesq approximation relies on the assumption that the normal Reynolds stresses are isotropic. This is a reasonable approximation[17] for small scale turbulence which is not under the influence of a wall, however, experimental studies of the wakes behind HATTs has shown that a high level of anisotropy is present[11]. In addition to this, a weakness of all RANS models is that they attempt to model the effect of turbulence on the mean flow, rather than the turbulent fluctuations themselves. This means that RANS models are less able to predict fluctuations in the forces on a turbine in a turbulent flow, information which is crucial for the correct structural design of a turbine. These and further details of the RANS approach can be found in [17].

An alternative approach to modelling turbulence is known as Large Eddy Simulation. This endeavours to distinguish between large eddies (which contain the majority of the turbulent kinetic energy, and tend to be more anisotropic[18]), which are directly resolved, and small eddies, which are modelled using a so-called Sub-Grid Scale model. In order to make this distinction, the unsteady Navier-Stokes equations are filtered in either physical or wavenumber space (in finite volume CFD, the local cell size makes a convenient spacial filter[17]).

LES has many advantages over RANS, including not relying on the assumption that turbulence at all length scales behaves in a universal manner (i.e. the large eddies are treated differently to the small eddies), and not assuming that the large scale turbulence and associated Reynolds stresses are isotropic. In addition to this, RANS turbulence models only provide information regarding the mean flow under the influence of turbulence, whereas LES yields information relating to both the instantaneous flow field, and, if the simulation is run for long enough, the mean flow field, allowing evaluations of the rate and magnitude of fluctuations. This information is of great interest in the structural design of HATTs, due to its influence on material fatigue. The disadvantage of LES when compared to RANS turbulence models is the great increase in computational expense, particularly when compared to two-equation RANS models. This is largely due to near-wall boundary layer regions. As the distance to a wall decreases, so the turbulent eddies reduce in size, which means that the largest scales, which are of most interest as they carry the largest proportion of turbulent kinetic energy, become much smaller than in the free-stream. To resolve all the length scales of interest, cell size must become much smaller than that required for RANS, with recommended values of  $y^+$  for LES of around  $y^+ = 1$ [19], compared to values of 400–500 for a  $k$ - $\omega$  SST RANS model[17].

In an attempt to combine the computational efficiency of RANS turbulence models (particularly in near-wall regions) with the extra information provided by LES turbulence models, hybrid RANS/LES models have been developed, such as Detached Eddy Simulation (DES)[20]. DES models recognise that, regardless of whether the Navier-Stokes equations are time-averaged (as is the case in RANS modelling), or spatially filtered (as with a finite-volume implementation of LES), the effect of turbulence at sub-grid scales is accounted for by

an eddy viscosity[19]. In DES, the turbulent length scale is compared to the local cell size to identify whether turbulence should be modelled using a RANS approach or if the turbulent length scales are large enough to allow the fluctuations to be resolved. The value of turbulent viscosity is then adapted appropriately, effectively using a RANS model where turbulent eddies are smaller than the local grid size (for example, in near wall regions) and recovering LES-like behaviour in regions where the local cell size allows the resolution of the turbulent fluctuations. This is done by modifying the turbulent kinetic energy dissipation rate in the following way[19]:

$$Y_k = \rho\beta^*k\omega \quad \text{becomes} \quad Y_k = \rho\beta^*k\omega F_{DES} \quad (2)$$

$$\text{where} \quad F_{DES} = \max\left(\frac{L_t}{C_{des}\Delta_{\max}}, 1\right) \quad (3)$$

With the turbulent length scale,  $L_t$  defined as:

$$L_t = \frac{\sqrt{k}}{\beta^*\omega}$$

When  $L_t \leq C_{des}\Delta_{\max}$ , then  $F_{DES} = 1$ , the turbulent kinetic energy dissipation term remains unmodified, and the model runs in ‘‘RANS mode’’. When  $L_t > C_{des}\Delta_{\max}$ , then  $F_{DES} \neq 1$ , and the turbulent kinetic energy dissipation term is modified. The extent of the modification is determined by the relative sizes of the turbulent length scale and the cell size, but generally, regions where  $F_{DES} \neq 1$  can be considered areas where the DES model is running in ‘‘LES mode’’.

In some cases with refined grids, the switch from RANS to DES can take place within the boundary layer, leading to premature flow separation[21], a phenomenon known as Grid-Induced Separation (GIS). In order to prevent this, shielding functions are provided in ANSYS Fluent in order to protect the boundary layer, ensuring that a RANS solution is applied and preventing the DES limiter from activating too soon. One of these schemes is known as ‘‘Delayed Detached Eddy Simulation’’ (DDES), is recommended by ANSYS[22], and is the scheme used for this work.

As noted by Ferziger in [17], there are situations in which LES may only require around twice the computational resources required by RSM. RSM, with its seven transport equations is employed when anisotropy of turbulence means that it is no longer appropriate to use the Boussinesq approximation. Since the wake behind a HATT has been shown to be highly anisotropic[11], the extra information that can be obtained by using DDES instead of an RSM model (i.e. the information relating to mean flow and the statistics of the resolved fluctuations) would justify the use of DDES over RSM, and over RANS models generally.

### B. Model geometry and boundary conditions

A 3 bladed, 10 m diameter turbine with nacelle and monopile stanchion was created inside a computational domain (see Figure 1). The blade profile is based on a Wortmann FX 63-137 profile, with approximately 30° twist from blade

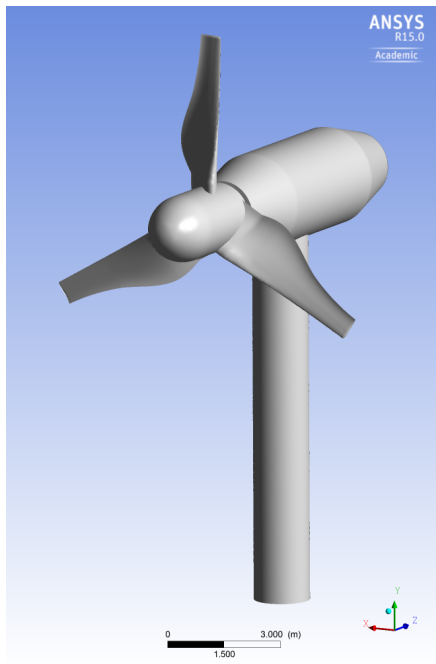


Fig. 1. The turbine modelled in this work

root to tip. Further details of the turbine geometry can be found in and [4] and [6]. The turbine axis was positioned at the origin, centred in the cross-stream direction, 30 m downstream of the domain inlet, and 11 m above the sea floor. The domain had dimensions of 280 m, 90 m and 45 m in the stream-wise ( $\hat{z}$ ), cross-stream ( $\hat{x}$ ) and vertical ( $\hat{y}$ ) directions. This represents an overall blockage ratio of 1.9% for the swept area, and the literature suggests that a blockage of this size has a negligible effect on the flow[23].

A sliding mesh scheme was used to simulate rotation of the turbine. This involves the creation of a cylindrical subdomain within the main fluid domain, aligned along the axis of rotation and encompassing the rotating elements of the turbine. A non-conformal mesh is created on the interface between the rotating cylinder and the main domain. The subdomain mesh is rotated with each timestep, simulating a rotational velocity of 2.25 rad/s, which when combined with the freestream velocity gives a Tip Speed Ratio (TSR) of 3.65, which previous studies have shown to yield maximum  $C_P$  for this turbine[6]. The rotating subdomain was meshed to a level of refinement comparable to that used by Morris[6], which was shown to be sufficient for a mesh independent flow solution using a  $k-\omega$  SST turbulence model. As the DDES model used in this work reverts to a  $k-\omega$  SST model in near-wall regions around the turbine, it is expected that this level of mesh resolution is sufficient for mesh independency in this region.

The main sea domain was further subdivided in order to improve mesh control and increase mesh density in the wake region. A cylinder aligned with the turbine axis and 15 m in diameter was created downstream of the nacelle, and extended to the downstream outlet of the main domain. This was meshed

using a sweep method, and was used to increase the mesh density in the wake region.

The turbine, nacelle and monopile, as well as the bottom boundary of the computational domain were all set to walls with a no-slip condition imposed on the flow. The sides and top of the domain were set to zero-shear or free-slip walls. The domain outlet was set as a pressure outlet with a gauge pressure of 0 Pa and the domain inlet was set to be a velocity inlet, with an average flow normal to the inlet boundary of 3.086 m/s (6 knots). In addition to a mean flow velocity at the inlet, a turbulence intensity was defined for each run and an integral length scale of 5 m was set. Turbulent perturbations were produced at the domain inlet using a vortex method based on the Biot-Savart law, with 1000 vortices[19]. These turbulence conditions were selected to approximate those measured at a potential tidal turbine site in the Sound of Islay[9].

A particle travelling at the free stream velocity would take 90.7 seconds to traverse the domain from inlet to outlet. A  $k-\omega$  SST model was run to produce an initial solution as a starting point for the DDES model. The transient RANS model was initially run for 1000 timesteps of 0.1 s representing a flow time of 100 s at which point the viscous model was changed to a DDES model and run for a further 4000 timesteps of 0.05 s, representing a further 200 s of flow time. Time sampling was carried out over the final 50 s (1000 timesteps) of this period to allow time averages to be taken after any transient effects from the DDES initialisation have had time to pass out of the domain.

In order to ensure that the turbulence model is recovering LES like behaviour in the detached regions, the DES turbulent kinetic energy dissipation multiplier was examined. This factor controls the switch from RANS to LES mode, with a value of  $F_{DES} = 1$  indicating full RANS modelling of turbulence, and full LES behaviour being recovered as  $F_{DES} \rightarrow \infty$ . In order to display the level of “resolvedness”, the value of  $1/F_{DES}$  is displayed in Figure 2 in the plane normal to  $\hat{y}$ , containing the turbine axis. Whilst this figure is taken from the TI = 3% case, the behaviour is the same for both the 7% and 10% case. A value of  $1/F_{DES} = 1$  corresponds to fully modelled turbulence (i.e. RANS mode), and  $1/F_{DES} = 0$  corresponds to full LES behaviour. Figure 2 shows the hybrid model to be running as desired, with near wall areas and the region around the turbine being modelled in RANS mode, and the turbulent kinetic energy dissipation term being modified in the wake region to recover LES-like behaviour. It should be noted that this plot is for an instantaneous value of  $1/F_{DES}$ , and the asymmetry in the plot is therefore due to the position of individual eddies at this particular timestep. The mesh density is symmetric about the centreline. The mesh density (when compared to rotor diameter) in the wake region is approximately the same as that used in previous studies using LES to examine wakes[14].

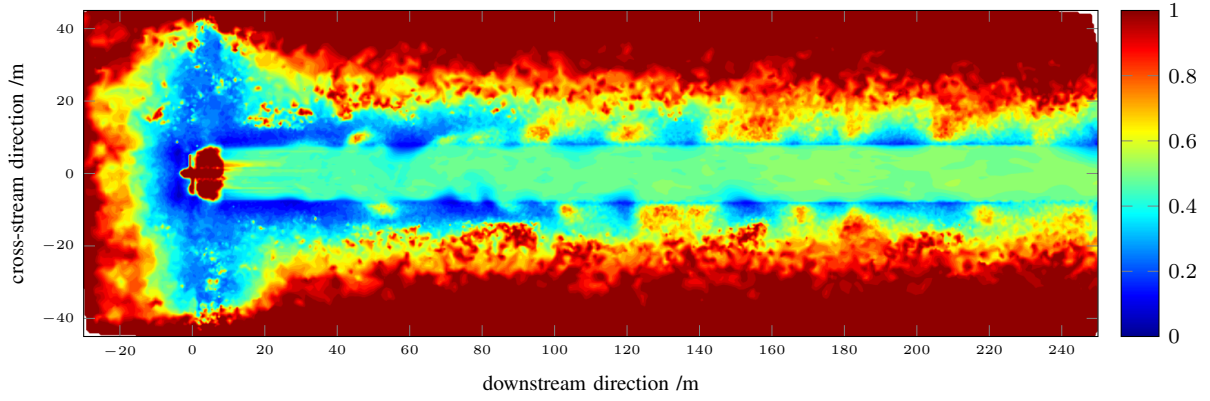


Fig. 2.  $1/F_{DES}$  at  $t = 300$  s for DDES,  $TI = 3\%$

### III. RESULTS

Results are presented for three different ambient turbulence conditions, with turbulent intensities of 10%, 7%, and 3% and length scale of 5 m. These broadly correspond to turbulence levels measured at a potential tidal energy site[9], as well as to the range of experimental results for three-bladed HATTs in [15] and [16]. Results for a RANS simulation ( $k-\omega$  SST) and DDES simulation are compared for each case. In addition to this, statistics for the performance characteristics of the turbine,  $C_P$ ,  $C_T$  and  $C_\theta$ , are analysed to allow comparison of the relative strengths of the two turbulence models in the prediction of both turbine wake and performance.

#### A. Performance prediction

The three performance characteristics that are examined in this work are the power coefficient,  $C_P$ , which shows the ratio of energy extracted by the turbine to the kinetic energy available in the free stream flow; the thrust coefficient,  $C_T$ , which shows the ratio of the thrust force on the turbine compared to a circular flat plate of the same diameter; and the torque coefficient,  $C_\theta$ , which shows ratio of torque generated by the turbine compared to the maximum theoretical torque. They are defined in the following way:

$$C_P = \frac{\tau\omega}{0.5\rho Av^3} \quad (4)$$

$$C_T = \frac{F_T}{0.5\rho Av^2} \quad (5)$$

$$C_\theta = \frac{\tau}{0.5\rho Av^2 r} \quad (6)$$

Whilst the turbine performance characteristics are not the main focus of this work on wakes, they are still important, as much of the experimental data to date has concentrated on and measured these characteristics, and RANS models have been shown to be able to predict these characteristics with a reasonable degree of accuracy in low turbulence flows[6]. A new viscous model, such as the DDES model used in this work, should show agreement with experimental and RANS

TABLE I  
COMPARISON OF PERFORMANCE CHARACTERISTICS WITH DIFFERENT TURBULENT INTENSITIES AND TURBULENCE MODELS

		TI = 3%	TI = 7%	TI = 10%
RANS	$\overline{C_P}$	0.435 (0.00087)	0.432 (0.00082)	0.426 (0.00086)
	$\overline{C_T}$	0.866 (0.00105)	0.865 (0.00092)	0.861 (0.00097)
	$\overline{C_\theta}$	0.119 (0.00026)	0.118 (0.00023)	0.117 (0.00024)
DDES	$\overline{C_P}$	0.465 (0.0086)	0.479 (0.035)	0.490 (0.054)
	$\overline{C_T}$	0.903 (0.0095)	0.917 (0.038)	0.929 (0.062)
	$\overline{C_\theta}$	0.128 (0.0023)	0.131 (0.0097)	0.134 (0.015)

results for turbine performance characteristics. The following results for  $C_P$ ,  $C_T$  and  $C_\theta$  have been obtained by interrogating the Fluent CFD results, extracting the moments on the blades and hub for the calculation of  $C_P$  and  $C_\theta$ , and extracting the force in the axial ( $z$ ) direction on the blades and hub for the calculation of  $C_T$ .

The mean results for  $C_P$ ,  $C_T$  and  $C_\theta$  are shown in Table I. The standard deviation of each of the means is shown in parenthesis. This table compares results from a RANS ( $k-\omega$  SST) model to a DDES model with the same boundary conditions. Performance statistics for the RANS model have been derived from a series of six equally spaced samples over a period of 25 s of flow time, from  $t = 275$  s to  $t = 300$  s. The results for the DDES models have been extracted from the CFD results using 21 equally spaced samples over a period of 50 s of flow time, from  $t = 250$  s to  $t = 300$  s. The mean and standard deviations of these samples are shown in Table I.

Experimental results[6],[7] have shown that the  $C_P$  of this turbine for this Tip Speed Ratio (TSR) in low turbulence flow conditions ( $TI=5\%$  and unstated integral length scale) is approximately 0.43. The RANS results presented in table I match this closely. The RANS results show a slight decrease in  $C_P$  with increasing turbulence intensity, which is in accordance

with the trend found in experimental studies[15]. The standard deviation in these results is very small, and remains almost constant, despite a change in turbulence intensity.

Table I also shows the results for the DDES simulations. It can be seen that the magnitude of the mean of all performance characteristics has increased, and the standard deviation has increased by between one and two orders of magnitude, indicating much larger fluctuations in the performance values. As might be expected, these fluctuations are largest in the most turbulent case (TI=10%), reflecting large turbulent features passing through the turbine.

### B. Wake prediction

The wake of an object in a flow is a region of disturbed flow downstream of the object. It is typically characterised by a fluid region with a lower overall velocity and an increased level of turbulence due to shed vortices. As the downstream distance from the object increases, so the surrounding flow mixes with the lower velocity wake, causing entrainment of energy and the recovery of the velocity in the wake region, until eventually the free stream velocity is regained. The rate at which this recovery occurs downstream of the turbine is of great interest to designers of turbine arrays, as it is a critical parameter in determining the optimal stream-wise turbine spacing.

In order to examine the rate of velocity recovery in the wake of the HATT, the following procedure was carried out: For the DDES results, flow in the  $\hat{z}$  direction was time-averaged over 50 s of flow time, from  $t = 250$  s to  $t = 300$  s. This allows mean results for velocity to be taken once transient flow effects from the initialisation and running-up of the simulation have settled. Results were extracted from the mean flow field on planes normal to the  $\hat{z}$  direction, at 10 m downstream intervals, between  $z = 20$  m and  $z = 250$  m from the turbine. For the RANS models, results were taken from the final timestep ( $t = 300$  s), using the same downstream planes and volumetric averaging procedure. Volumetric averages of mean (time averaged) velocity in the  $\hat{z}$  direction were taken over the swept area of the turbine at 10 m intervals downstream of the origin, and the results of this are presented in Figure 4, with downstream distances normalised against turbine diameter, and stream wise velocity normalised against the free stream velocity. To allow visualisation of the different kind of information obtained using DDES over RANS turbulence models, three diagrams showing averaged and instantaneous flow fields for a DDES model as well as the flow field for a RANS model are presented in Figure 3.

## IV. DISCUSSION

For the RANS results, the mean predicted values of  $C_P$ ,  $C_T$  and  $C_\theta$  show good agreement with previous studies[6],[7], for both simulation and low-turbulence flume experiments. In addition to this, they follow trends from experimental work on other HATTs[15], with a slight decrease in  $C_P$  with increasing ambient turbulence intensity. The RANS results, however, show a much lower intensity of fluctuations than those found

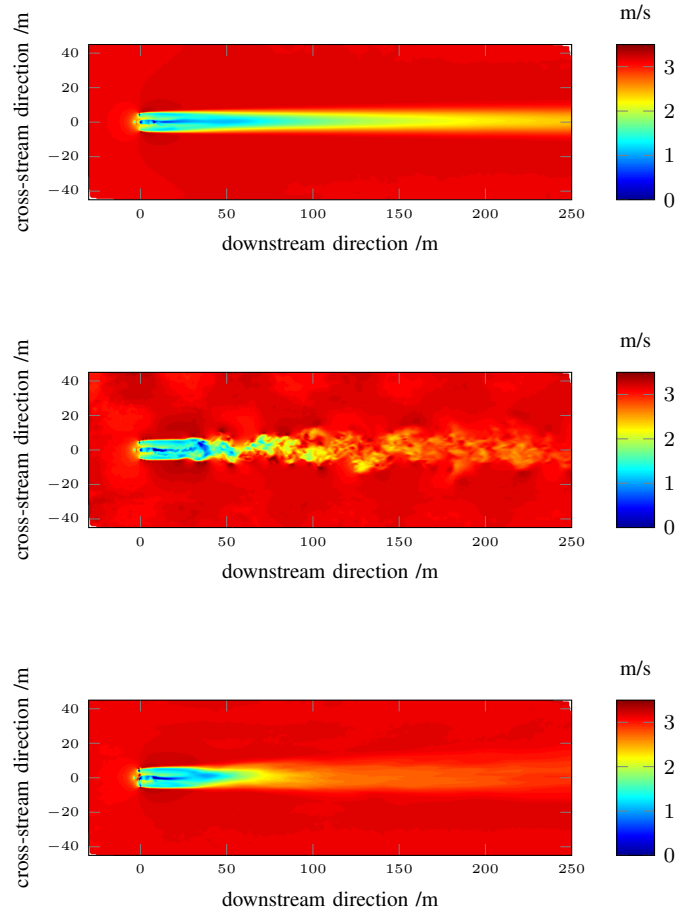


Fig. 3. Comparison of velocity in the  $\hat{z}$  direction for the two different turbulence models with 3% ambient turbulence intensity. Top is RANS model, middle is instantaneous velocity from the DDES model, bottom is time averaged over 50 s for DDES

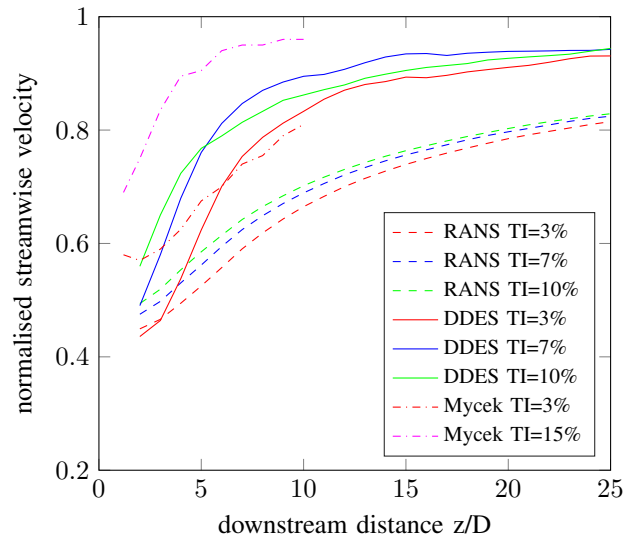


Fig. 4. Wake recovery, including experimental results from [16].

experimentally in [15], and show almost no change despite a change in turbulence intensity.

Performance data for the DDES models shows a significant increase in the mean values of  $C_P$ ,  $C_T$  and  $C_\theta$ , with the most extreme cases showing an increase of up to 10% when compared to values measured in low turbulence flume experiments. Much greater is the increase in the standard deviation of the data of one or two orders of magnitude, indicating much larger fluctuations in the performance characteristics. These show good agreement with the fluctuations measured experimentally in [15], suggesting that the turbulent fluctuations may be better modelled by the DDES model than the RANS model. It was also noted in [15] that, whilst increasing turbulence intensity has a detrimental effect on  $C_P$ , a larger turbulent length scale tends to have a positive effect on  $C_P$ , and the effect of increasing length scale outweighs that of increasing turbulence intensity. It is expected that the scale resolving properties of the DDES model will more accurately reproduce the large length scale turbulence than the RANS models, and it could be that more accurate modelling of large scale turbulence is outweighing the effects of increasing the turbulence intensity. Large scale turbulent fluctuations appear to the turbines as surges, and on subsequent examination the fluctuations in the performance of the turbines have been found to correspond in time to surges in the flow passing through the turbine.

Additionally,  $C_P$ ,  $C_T$  and  $C_\theta$  as well as TSR quoted in this work are referenced to the free-stream inlet velocity of 3.086 m/s. Large fluctuations will tend to increase the energy contained in the flow through the turbine. It has been argued that, as the equations 4, 5 and 6 contain either  $v^2$  or  $v^3$ , this operation should take place before averaging over the area of the disc [15]. Using the free stream velocity will tend to *under predict* the available energy in a non-uniform flow, due to the the squaring or cubing procedure. This effect will increase as the magnitude of the fluctuations increases and tend to *over predict* the value of  $C_P$ . This could also be a factor in explaining the higher values of turbine performance data for the DDES model. This is a problem which highlights a weakness in the standard definitions of  $C_P$ ,  $C_T$  and  $C_\theta$  when applied to inhomogeneous flows which change in time. The flow field which would be present in the plane of the turbine can never be truly measured, as it is directly influenced by the presence of a turbine. For realistic turbulent flows therefore it may be more helpful to accept  $C_P$ ,  $C_T$  and  $C_\theta$  referenced to the free stream averaged velocity as useful rules-of-thumb to assist in the characterisation of turbines, rather than as performance indicators which are expected to be precisely met by a turbine in a realistic flow.

Figure 4 shows data for RANS models, DDES models and experimental results from [16] for TI=3% and TI=15% cases. The experimental results are taken from a study of the performance and wake of a 3 bladed, 0.7 m HATT at the IFREMER flume tank in Boulogne-Sur-Mer. Whilst the geometry of the turbine in the experimental case is not the same as that of the numerical model used here, [16] has been used as it represents one of the most comprehensive studies of

HATT wakes to date, and includes detailed descriptions of the ambient turbulence conditions. It can be seen that the RANS models follow the expected trend, with velocity recovery in the wake occurring more quickly for higher ambient turbulence intensity levels. The RANS cases do, however, appear to significantly under predict the overall rate of velocity recovery, showing 80% velocity recovery at approximately  $z/D = 18$  downstream of the turbine for the 10% case, whereas even the 3% turbulence intensity experimental case demonstrates 80% recovery by  $z/D = 10$ .

In contrast, the DDES results appear to more accurately reproduce the experimental data for the limited range of data available. The DDES results (and indeed the experimental data) show a sharp initial recovery, followed by a much more gradual rate of recovery, whereas the RANS data suggests a more consistent and gradual recovery over a larger downstream distance. The curve showing the fastest wake recovery is the experimental TI=15% case from [16], which has a turbulence intensity higher than any of the CFD models. Whilst all three DDES models run here show wake recovery closer to the experimentally measured wakes, it should be noted that the expected trend of faster recovery for higher turbulence intensity cases is only reproduced in the near wake region. Beyond approximately  $z/D = 5$  downstream, the DDES TI=7% case shows increased wake recovery when compared to the DDES TI=10% case, and whilst the difference is small (approximately 3%), at the time of writing, further work is being undertaken to determine the cause of this difference.

Figure 3 shows visually the different types of data gained from DDES simulations when compared to the RANS simulation. The differences between the results gained from a RANS simulation and DDES are striking. With the RANS models, it is possible to obtain information regarding the effects on the mean flow field due to the presence of the turbine, but not regarding the interaction of individual turbulent fluctuations with the wake. The instantaneous DDES flow field seems to indicate that the wake behind a HATT persists for approximately four diameters downstream before starting to be broken up due to interactions with the free stream. This area of wake break-up is characterised by large turbulent features which persist until approximately 13 diameters downstream of the turbine, where they become much smaller and the flow becomes more evenly mixed. Whilst this demonstrates the increase in information that can be gained using a DDES model, it is expected that the ambient turbulence produced for the simulation must also accurately reflect that which is to be expected at a given turbine site.

## V. CONCLUSIONS AND PROSPECTS

This work has shown that whilst a k- $\omega$  SST RANS turbulence model can produce accurate predictions for important turbine performance characteristics, it shows significant weakness when predicting the length and character of the wake, which appears to be better modelled in DDES. RANS models do show significant advantages in the length of time required to run a simulation, taking approximately one-half to

one-third of the time required for an equivalent DDES model. DDES models do, however, provide more information about the wake, giving not only time-averaged results similar to the type gained from RANS model, but also information regarding the magnitude and rate of turbulent fluctuations – information of vital importance to engineers considering placing turbines in flow affected by upstream turbines (for example, in an array).

Future work is envisioned to refine the use of the DDES model, and to examine its ability to model the effects of different turbulent length scales on the wake of a HATT. In addition to this, experimental work for the particular turbine studied here is required for model validation.

This initial study has highlighted some areas for further study, and indicated that accepted norms for the assessment of turbine performance might require revision in light of the challenges presented by the analysis of turbines in highly turbulent flows. An ability to model flows with turbulent features with a length scale similar to the size of the turbine is expected to be of great value. Fluctuations in forces on the turbine will be of interest to structural engineers, but beyond this fluctuations in effective TSR will be of interest to those designing control systems such as active blade pitch control for performance optimisation.

#### ACKNOWLEDGEMENTS

The authors acknowledge the financial support provided by the Welsh Government and Higher Education Funding Council for Wales through the Sêr Cymru National Research Network for Low Carbon, Energy and the Environment.

#### REFERENCES

- [1] Sustainable Development Commission. Turning the tide, 2007. <http://www.sd-commission.org.uk/publications.php?id=607>.
- [2] Ross Vennell, Simon W. Funke, Scott Draper, Craig Stevens, and Tim Divett. Designing large arrays of tidal turbines: A synthesis and review. *Renewable and Sustainable Energy Reviews*, 41:454–472, 2015.
- [3] J. Schluntz and R.H.J. Willden. The effect of blockage on tidal turbine rotor design and performance. *Renewable Energy*, 81:432–441, 2015.
- [4] A. Mason-Jones, D.M. O’Doherty, C.E. Morris, T. O’Doherty, C.B. Byrne, P.W. Prickett, R.I. Grosvenor, I. Owen, S. Tedds, and R.J. Poole. Non-dimensional scaling of tidal stream turbines. *Energy*, 44:820–829, 2012.
- [5] C.E. Morris, D.M. O’Doherty, A. Mason-Jones, and T. O’Doherty. Evaluation of the swirl characteristics of a tidal stream turbine wake. *International Journal of Marine Energy*, 14:198–214, 2016.
- [6] Ceri Morris. *Influence of Solidity on the Performance, Swirl Characteristics, Wake Recovery and Blade Deflection of a Horizontal Axis Tidal Turbine*. PhD thesis, School of Engineering, Cardiff University, 2014.
- [7] A. Mason-Jones. *Performance assessment of a Horizontal Axis Tidal Turbine in a high velocity shear environment*. PhD thesis, School of Engineering, Cardiff University, 2010.
- [8] Ali M. AbdelSalam and Velraj Ramalingam. Wake prediction of horizontal-axis wind turbine using full-rotor modeling. *J. Wind Eng. Ind. Aerodyn.*, 124:7–19, 2014.
- [9] I.A. Milne, R.N. Sharma, R.G.J. Flay, and S. Bickerton. Characteristics of the turbulence in the flow at a tidal stream power site. *Phil Trans R Soc A*, 371:20120196, 2013.
- [10] Paul Mycek, Benoît Gaurier, Grégory Germain, Grégory Pinon, and Elie Rivoalen. Experimental study of the turbulence intensity effects on marine current turbines behaviour. part II: Two interacting turbines. *Renewable Energy*, 68:876–892, 2014.
- [11] S.C. Tedds, I. Owen, and R.J. Poole. Near-wake characteristics of a model horizontal axis tidal stream turbine. *Renewable Energy*, 63:222–235, 2014.
- [12] Paul Mycek, Benoît Gaurier, Grégory Germain, Grégory Pinon, and Elie Rivoalen. Numerical and experimental study of the interaction between two marine current turbines. *International Journal of Marine Energy*, 1:70–83, 2013.
- [13] H. Sarlak, C. Meneveau, and J.N. Sørensen. Role of subgrid-scale modeling in large eddy simulation of wind turbine wake interactions. *Renewable Energy*, 77:386–399, 2015.
- [14] T. Blackmore, W.M.J. Batten, and A.S. Bahaj. Influence of turbulence on the wake of a marine current turbine simulator. *Proc. R. Soc. A*, 470:20140331, 2014.
- [15] Tom Blackmore, Benoît Gaurier, Luke Myers, Gregory Germain, and AbuBakr S Bahaj. The Effect of Freestream Turbulence on Tidal Turbines. In *Proceedings of the 11th European Wave and Tidal Energy Conference, Nantes, France*, 6–11th Sept 2015.
- [16] Paul Mycek, Benoît Gaurier, Grégory Germain, Grégory Pinon, and Elie Rivoalen. Experimental study of the turbulence intensity effects on marine current turbines behaviour. part I: One single turbine. *Renewable Energy*, 66:729–746, 2014.
- [17] H.K. Versteeg and W. Malalasekera. *An Introduction to Computational Fluid Dynamics, The Finite Volume Method*. Pearson Education Limited, 2007.
- [18] H. Tennekes and J.L. Lumley. *A First Course in Turbulence*. The MIT Press, 1972.
- [19] ANSYS. *ANSYS Fluent Theory Guide*, November 2013. Release 15.0.
- [20] P.R. Spalart, W-H. Jou, M.Strelets, and S.R. Allmaras. Comments on the feasibility of LES for wings, and on a hybrid LES/RANS approach. In Chaoqun Liu and Zhining Liu, editors, *Proceedings of the First AFOSR International Conference on DNS/LES*, pages 137–147. Greyden Press, 1997.
- [21] F. R. Menter, M. Kuntz, and R. Langtry. Ten Years of Industrial Experience with the SST Turbulence Model. In K. Hanjalić, Y. Nagano, and M. Tummers, editors, *Turbulence, Heat and Mass Transfer 4*. Begell House, Inc., 2003.
- [22] ANSYS. *ANSYS Fluent User’s Guide*, November 2013. Release 15.0.
- [23] Robert Howell, Ning Qin, Jonathan Edwards, and Naveed Durrani. Wind tunnel and numerical study of a small vertical axis wind turbine. *Renewable Energy*, 35:412–422, 2010.